124
1-12-81
LA-8388
R1083
Dr. 2187

MASTER

Space-Charge Limits in Linear Accelerators

University of California

LOS ALAMOS SCIENTIFIC LABORATORY
Post Office Box 1663 Los Alamos, New Mexico 87545

SPACE-CHARGE LIMITS IN LINEAR ACCELERATORS

by

Thomas P. Wangler

ABSTRACT

This report presents equations that allow an approximate evaluation of the limiting beam current for a large class of radio-frequency linear accelerators, which use quadrupole strong focusing. Included are the Alvarez, the Wideröe, and the radio-frequency quadrupole linacs. We obtain the limiting-current formulas for both the longitudinal and the transverse degrees of freedom by assuming that the average space-charge force in the beam bunch arises from a uniformly distributed charge within an azimuthally symmetric three-dimensional ellipsoid. The Mathieu equation is obtained as an approximate, but general, form for the transverse equation of motion. The smooth-approximation method is used to obtain a solution and an expression for the transverse current limit. The form of the current-limit formulas for different linac constraints is discussed.

I. INTRODUCTION

Maschke[1] obtained current-limit formulas for a linear accelerator by assuming spherical beam bunches and by applying the thin-lens approximation to represent the quadrupole focusing. Much previous work has been done using the three-dimensional ellipsoid model, which has been reviewed by Gluckstern.[2] In this report we use the three-dimensional ellipsoid model to approximate the beam bunch in a linear accelerator. Then we derive a transverse equation of motion in the form of the Mathieu equation, which has approximate validity for a variety of linac configurations with quadrupole focusing, including the Alvarez and Wideröe linacs with both the FODO and the FOFODODO polarity groupings and the radio-frequency quadrupole (RFQ) linac.[3] For the RFQ, which provides a continuously distributed radial focusing force, this approach should be more applicable than the thin-lens approximation. Transverse and longitudinal current-limit formulas are obtained from a smooth approximation. These equations are intended to provide a useful guide for estimating the beam-current capacity in a linear accelerator, but not as a substitute for a more detailed computer simulation.

In Sec. II we derive the transverse limits; in Sec. III we obtain longitudinal limits. Section IV contains a discussion of the application of the formulas. Appendix A contains a brief review of the results of the three-dimensional ellipsoid model. Appendix B gives some Mathieu equation properties. Appendix C summarizes the notation used in this report.

II. TRANSVERSE SPACE-CHARGE LIMIT

We use a model of a uniform charge distribution within a three-dimensional ellipsoid to represent the space-charge force within a beam bunch, (Appendix A), but we do not include the interactions between bunches. The equation of motion for x is

$$\frac{1}{\beta\gamma}\frac{d}{ds}\left[\beta\gamma\frac{dx}{ds}\right]+\left[k_t^{\,2}+\frac{\pi eq E_0 T\sin\phi}{m_0c^2\lambda\beta^3\gamma^3}-\frac{3Z_0 eqI\lambda[1-f(p)]}{8\pi m_0c^2r^2b\beta^2\gamma^3}\right]x=0\ . \tag{1}$$

A similar equation can be written for y. The last term in Eq. (1) is the space-charge term. Here I is the beam current in amperes averaged over a radio-frequency (rf) period assuming all buckets are filled, $Z_0 = 376.73\,\Omega$ is the free-space impedance, r and b are the transverse and longitudinal semiaxes of the ellipsoid, and f(p) is the ellipsoid form factor given in Appendix A. The beam bunch will be represented by an ellipsoid, whose dimensions are averaged over a focusing period. The effective ellipsoid is therefore azimuthally symmetric about the beam axis. The quantity k_t, which has the dimensions of wave number, represents the quadrupole focusing term and is assumed to be a periodic function of s. Within the focusing elements, it can be expressed as

$$k_t^{\,2}=\begin{cases}\pm\dfrac{eqB}{m_0\beta\gamma ca} & ;\ \text{magnetic quadrupoles}\\[2ex] \pm\dfrac{eqV}{m_0\beta^2\gamma c^2a^2} & ;\ \text{electric quadrupoles}\end{cases}\ , \tag{2}$$

where a is the semiaperture, B is the pole-tip magnetic field, and V is the voltage between adjacent poles. The second term within the brackets of Eq. (1) represents the first-order radial-force effect associated with the presence of the linac rf longitudinal field. We express the period of the focusing elements as

$$L = N\beta\lambda \ . \tag{3}$$

The quantity N depends upon the type of linac and upon the polarity grouping of the focusing elements, and is given in Table I. For the Wideröe linacs we assume that quadrupole magnets are placed only in the grounded (alternate) drift tubes, whereas for the Alvarez linacs we assume that every drift tube contains a quadrupole.

Now we will assume that the fractional change of $\beta\gamma$ is small over a transverse oscillation period. We make a Fourier expansion of the function k_t^2. For convenience we take the origin s = 0 to be midway between focusing elements of opposite polarity so that k_t^2 is an odd function of s. We introduce the dimensionless variable η where

$$\eta = s/L \ . \tag{4}$$

TABLE I

N FOR DIFFERENT LINAC CONFIGURATIONS

Linac Types	Polarity Grouping	N
RF Quadrupole	FD	1
π-π Wideröe	FODO	2
π-π Wideröe	FOFODODO	4
π-3π Wideröe	FODO	4
π-3π Wideröe	FOFODODO	8
Alvarez	FODO	2
Alvarez	FOFODODO	4

Then we can write

$$k_t^2(\eta) = \sum_{m=1}^{\infty} b_m \sin 2\pi m\eta \quad , \tag{5}$$

where

$$b_m = 2 \int_{-\frac{1}{2}}^{+\frac{1}{2}} k_t^2(\eta) \sin 2\pi m\eta d\eta \quad . \tag{6}$$

Equation (1) then becomes

$$\frac{d^2x}{d\eta^2} + \left[L^2 \sum_{m=1}^{\infty} b_m \sin 2\pi m\eta + \Delta \right] x = 0 \quad , \tag{7}$$

where

$$\Delta = \Delta_{rf} + \Delta_{sc} \quad , \tag{8}$$

$$\Delta_{rf} = \frac{\pi e q E_0 T \sin \phi_s \lambda N^2}{m_0 c^2 \beta \gamma^3} \quad , \tag{9}$$

and

$$\Delta_{sc} = \frac{-3Z_0 e q I \lambda^3 N^2 [1 - f(p)]}{8\pi m_0 c^2 \gamma^3 r^2 b} \quad . \tag{10}$$

In Eq. (9) we made the approximation of replacing the phase ϕ with the synchronous phase ϕ_s. We do not neglect the rf defocus parameter Δ_{rf}, which can become important either for low velocities or for high accelerating fields. We now assume a hard-edged model for the focusing quadrupoles, so that the field strength is constant within a quadrupole and zero outside. This hard edged model is applicable for focusing provided in conventional linacs, but does not apply for the RFQ structure, which we will discuss separately. We assume that all quadrupoles within a focusing period are of the same length and are equally spaced. We introduce a filling factor Λ, which we define as the fraction of the focusing period that contains quadrupole elements. For the FODO polarity grouping, the Fourier coefficents are

$$b_m = \begin{cases} \dfrac{4|k_t^2|}{\pi m} \sin \dfrac{m\pi}{2} \sin \dfrac{m\pi\Lambda}{2} & ; \text{ m odd} \\ 0 & ; \text{ m even} \end{cases} . \tag{11}$$

For the FOFODODO case we obtain

$$b_m = \begin{cases} \dfrac{+8|k_t^2|}{\sqrt{2}\, m\pi} \sin \dfrac{m\pi\Lambda}{4} & ; m = 1,3,9,11,... \\ \dfrac{-8|k_t|^2}{\sqrt{2}\, m\pi} \sin \dfrac{m\pi\Lambda}{4} & ; m = 5,7,13,15,... \\ 0 & ; \text{ m even} \end{cases} . \tag{12}$$

To obtain simple equations, we now ignore all terms in the expansion of Eq. (7) except for the leading m = 1 term. Then we obtain

$$\frac{d^2x}{d\eta^2} + \left[\theta_0^2 \sin 2\pi\eta + \Delta \right] x = 0 , \tag{13}$$

where from Eqs. (2), (5), (6), (11), and (12) we have

$$\theta_0^2 = \begin{cases} \dfrac{eqV\lambda^2N^2\chi}{m_0c^2\gamma a^2} & ; \text{ electric quadrupoles} \\ \dfrac{eqB\lambda^2N^2\beta\chi}{m_0c\gamma a} & ; \text{ magnetic quadrupoles} \end{cases} , \tag{14}$$

where χ is a focusing efficiency factor given by

$$\chi = \begin{cases} \dfrac{4}{\pi} \sin \dfrac{\pi\Lambda}{2} & ; \text{ FODO} \\ \dfrac{8}{\sqrt{2}\pi} \sin \dfrac{\pi\Lambda}{4} & ; \text{ FOFODODO} \end{cases} \tag{15}$$

Equation (13) also describes the transverse motion in the RFQ.[4] The electric quadrupole value for θ_0^2, given by Eq. (14), can be used for the RFQ if N = 1 and if χ is interpreted as the focusing efficiency parameter given in Ref. 3.

Equation (13) has the form of the Mathieu equation. In the smooth approximation the solution is[5]

$$x = X(\eta)\ \left(\beta_x(\eta)\right)^{1/2} \quad , \tag{16}$$

where $X(\eta)$ varies slowly over a focusing period and $\beta_x\ (\eta)$ is the periodic betatron function, which has the same period as the focusing elements. The function $X(\eta)$ satisfies the equation

$$\frac{d^2X}{d\eta^2} + \sigma^2 X = 0 \quad , \tag{17}$$

where σ is the smoothed phase advance per focusing period given by

$$\sigma^2 = \frac{\theta_0^{\ 4}}{8\pi^2} + \Delta \quad . \tag{18}$$

The solution to Eq. (17) can be written as

$$X \propto \cos\ (\sigma\eta + \delta) \quad . \tag{19}$$

The betatron function in this approximation can be expressed as

$$\beta_x(\eta) = \frac{L}{\sigma}\left[1 + \frac{\theta_0^{\ 2}}{(2\pi)^2}\ \sin\ 2\pi\eta\right]^2 \tag{20}$$

and the beam envelope radius r_x can be related to the emittance ε and the betatron function by

$$r_x^{\ 2} = \varepsilon\beta_x \quad . \tag{21}$$

From Eq. (18) we may write

$$\sigma^2 = \sigma_0^{\ 2}\left(1 - \mu_t\right) \quad , \tag{22}$$

where σ_0 is the phase advance per focusing period for zero current given by

$$\sigma_0^{\ 2} = \frac{\theta_0^{\ 4}}{8\pi^2} + \Delta_{rf} \tag{23}$$

and μ_t is discussed below. The Mathieu equation stability diagram, (Appendix B) becomes a universal stability diagram for all the linacs discussed in this paper.

The transverse space-charge parameter μ_t is the ratio of the space-charge force to the smoothed focusing force and is given by

$$\mu_t = \frac{-\Delta_{sc}}{\sigma_0^2} \quad . \tag{24}$$

If we substitute Eq. (10) into Eq. (24) and solve for the current, we obtain

$$I = \frac{8\pi}{3Z_0} \mu_t \frac{m_0 c^2}{eq} \frac{\gamma^3 r^2 b \sigma_0^2}{N^2 \lambda^3 [1 - f(p)]} \quad . \tag{25}$$

We assume that the radius r of the ellipsoid representing the bunch is given by the geometric mean of the maximum and minimum semiaxes r_+ and r_- over a focusing period. Thus

$$r^2 = r_+ r_- = \frac{r_+^2}{\psi} \quad , \tag{26}$$

where ψ is the envelope modulation factor given from Eq. (20) and (21) by

$$\psi = \frac{r_+}{r_-} = \frac{\left[1 + \left(\frac{\theta_0}{2\pi}\right)^2\right]}{\left[1 - \left(\frac{\theta_0}{2\pi}\right)^2\right]} \quad . \tag{27}$$

Notice that ψ does not depend upon the beam current.

As the beam current increases, the radius of the beam bunch also increases, and eventually the beam will be limited by the aperture. Thus, at the current limit, we assume

$$r_+ = a \quad . \tag{28}$$

From Eq. (20) we can obtain an expression for the geometric mean of the maximum and minimum of the betatron function, which is approximately

$$\bar{\beta}_x = \left(\beta_+ \beta_-\right)^{1/2} \cong \frac{L}{\sigma} \quad . \tag{29}$$

To estimate the bunch length 2b at the transverse current limit, we assume that the bunch is also near the longitudinal current limit. Then a bunch length that is consistent with other studies[2] for beams near the longitudinal limit is

$$b = \beta\lambda \frac{|\phi_s|}{2\pi} \quad . \tag{30}$$

Because μ_t is the ratio of the space-charge to the focusing force, we would expect physically that μ_t should not exceed approximately $\mu_t = 1$ for stable motion. Recent numerical studies[6] suggest that in the presence of space charge, the necessary requirements for stable motion in a linear accelerator without large emittance growth are

$$\sigma_0 \lesssim \pi/2 \tag{31}$$

and

$$\frac{\sigma}{\sigma_0} \gtrsim 0.4 \quad . \tag{32}$$

We recognize that future studies may modify the best estimates for these numbers. The limit given by Eq. (32) can be combined with Eq. (22) to yield a maximum for the space-charge parameter given by

$$\mu_t = 1 - \left(\frac{\sigma}{\sigma_0}\right)^2_{min} = 0.84 \quad , \tag{33}$$

where

$$\left(\sigma/\sigma_0\right)_{min} = 0.4 \quad . \tag{34}$$

As the limit given by Eq. (34) is approached by increasing the beam current, a large emittance growth rate will lead to an increase in the beam size and beam losses will occur when the beam hits the aperture. We assume that the transverse current limit is determined by this effect. Then, if we substitute Eqs. (26), (28), and (30) into Eq. (25) we obtain

$$I_t = \frac{4\mu_t m_0 c^2 \beta\gamma^3 |\phi_s| \sigma_0^{\,2}}{3 z_0 e q N^2 \psi [1 - f(p)]} \left(\frac{a}{\lambda}\right)^2 \quad , \tag{35}$$

where μ_t is given by Eq. (33) and σ_0 is given by Eq. (23), but should not exceed the approximate limit given by Eq. (31).

Equation (35) is the desired transverse current-limit formula. It shows the dependence of the maximum beam current upon the linac parameters. However, if additional constraints are imposed upon these parameters as they vary, it is useful to express the current limit explicitly in terms of these constrained quantities. The form taken by the equations will look entirely different when different constraints are applied. This was emphasized by Reiser[7] in connection with the scaling of beam-transport current limits. A discussion of two important constraints follows.

Case 1: Let us assume that the maximum phase advance $\sigma_0 = \pi/2$ is always maintained. Equation (35), which explicitly contains σ_0, already is in a convenient form to show how the current depends upon the other parameters when σ_0 is held fixed.

According to Eq. (35), increasing the value of a/λ will increase the limiting current. However, as a/λ increases in a linac, the magnitude of the on-axis accelerating field decreases. This effect is sometimes described as a reduction in transit-time factor. The on-axis transit-time factor T is given by Eq. (50) in Sec. III. A reduction in T causes an undesirable reduction in the rate of acceleration and, as we will see later, in the longitudinal current limit. If we assume somewhat arbitrarily that the maximum acceptable aperture is

$$a = \frac{\beta\lambda}{10} , \qquad (36)$$

we can get an estimate for the magnitude of the current given by Eq. (35). To estimate the envelope modulation factor ψ when $\sigma_0 = \pi/2$, let us ignore the rf defocus parameter in Eq. (23). Then from Eq. (27) we get

$$\psi = 2.1 . \qquad (37)$$

Given Eqs. (30) and (36), the choice $|\phi_s| = 2\pi/10$ and $f(p) = 1/3$ corresponds to a spherical bunch. These substitutions into Eq. (35) yield for an ion of mass number A_n the expression

$$I = 3.65 \times 10^4 \mu_t \left(\frac{A_n}{q}\right) \frac{(\beta\gamma)^3}{N^2} \quad \text{[amperes]}. \qquad (38)$$

This is of the same form as Maschke's result,[1] which was derived for a spherical bunch using a thin-lens approximation for the focusing. Our coefficient is smaller than his because of our use of average rather than instantaneous current.

Case 2: We now assume that practical upper limits on the focusing fields prevent the phase advance σ_0 from reaching its maximum limiting value, and that the focusing field itself is constrained to equal some specified maximum practical value. By substituting Eqs. (14) and (23) into Eq. (35), we can show that for magnetic-quadrupole focusing

$$I_t = \frac{\mu_t c^2}{6\pi^2 Z_0} \left(\frac{eq}{m_0 c^2}\right) \frac{\beta^3 \gamma |\phi_s| (\lambda N \chi B)^2}{\psi[1 - f(p)]} \left[\frac{\theta_0^4 + 8\pi^2 \Delta_{rf}}{\theta_0^4}\right] . \tag{39}$$

For electric-quadrupole focusing we obtain

$$I_t = \frac{\mu_t}{6\pi^2 Z_0} \left(\frac{eq}{m_0 c^2}\right) \frac{\beta \gamma |\phi_s| (\lambda N \chi)^2}{\psi[1 - f(p)]} \left(\frac{V}{a}\right)^2 \left[\frac{\theta_0^4 + 8\pi^2 \Delta_{rf}}{\theta_0^4}\right] . \tag{40}$$

If the rf defocus parameter is small, the last factor in brackets in Eqs. (39) and (40) is near unity. However, the rf defocus term can become important especially for applications at low velocities and at high accelerating fields. The most obvious differences between the case 1 current limit of Eq. (35) and the case 2 formulas of Eqs. (39) and (40) are in the charge-to-mass ratio dependence and in the dependence upon rf wavelength. Higher transverse current limits are obtained at lower frequencies for case 2.

Equation (40) is valid for the RFQ if N = 1 and if Δ_{rf} is evaluated from Eq. (9) using the results for the RFQ given in Ref. 3 that

$$E_0 = \frac{2AV}{\beta\lambda} , \tag{41}$$

where A is the acceleration efficiency parameter, and that for the synchronous particle

$$T = \frac{\pi}{4} . \tag{42}$$

The acceleration efficiency is typically about $A = 0.5$. The factor χ in Eq. (40) is the focusing efficiency also given for the RFQ in Ref. 3.

Two important approximations made in this treatment were the neglect of higher order terms in the Fourier expansion of the function k_t^2 for conventional linacs and the use of the smooth approximation. The absence of the higher order terms gave an equation of motion in the form of the Mathieu equation. The smooth approximation applied to this equation allows us to write some simple formulas for the important quantities that appear in the theory. As is discussed by Bruck[5] and Reiser,[7] the accuracy of the smooth approximation improves as the phase advance per focusing period decreases. Equation (23) is expected to be accurate to better than 10 to 15% for phase-advance values less than 90^0. Because of the limitation expressed by Eq. (34) and because the phase advance always decreases as the beam current increases, we expect that the smooth approximation will be satisfactory to obtain useful formulas.

Within the smooth approximation it is easy to study the effect of neglecting the higher order terms of the Fourier expansion. The results show that the accuracy decreases at very small values of the filling factor. However, for $0.1 \leq \Lambda \leq 1.0$ and both the FODO and FOFODODO cases, this assumption causes an error in the phase advance that is always less than about 16%. The combined effect of both assumptions can be tested using the example of the FODO polarity grouping at $\sigma_0 = 90^0$ and $\Lambda = 1/2$. When we compare the formulas in this paper with the exact results, we find that the phase advance calculated in this paper is in error by 11% and the beam envelope is in error by 17%. For smaller phase advances the accuracy will improve.

III. LONGITUDINAL SPACE-CHARGE LIMIT

The quasi-periodic rf electric force applied to the beam provides the longitudinal focusing. To a good approximation we can replace the real periodic forces by a continuously acting average force. From the three-dimensional ellipsoid model we write the smoothed longitudinal equation of motion[2] as

$$\frac{1}{(\beta\gamma)^3}\ \frac{d}{ds}\left[\beta^3\gamma^3\,\frac{d}{ds}\,\Delta\phi\right] + k_\ell^{\,2}\left[\left(1 - \mu_\ell\right)\Delta\phi - \frac{(\Delta\phi)^2}{2|\phi_s|}\right] = 0 \quad , \tag{43}$$

where $\Delta\phi$ is the particle phase relative to the synchronous phase ϕ_s. The longitudinal wave number is given by

$$k_\ell^{\,2} = \frac{-2\pi eqE_0T\sin\phi_s}{m_0c^2\lambda\beta^3\gamma^3} , \tag{44}$$

where E_0 is the average axial field amplitude and T is the transit-time factor.

The longitudinal space-charge parameter μ_ℓ is given by

$$k_\ell^{\,2}\mu_\ell = \frac{3Z_0eqI\lambda f(p)}{4\pi m_0c^2r^2b\beta^2\gamma^3} . \tag{45}$$

If we solve Eq. (45) for the current, we obtain

$$I_\ell = \frac{8\pi^2}{3Z_0}\,\mu_\ell\,\frac{r^2b}{f(p)}\,\frac{1}{\beta\lambda^2}\,E_0T\,|\sin\phi_s| . \tag{46}$$

As in the transverse case, because μ_ℓ is the ratio of the space-charge force to the focusing force, we would expect physically that μ_ℓ should not exceed approximately $\mu_\ell = 1$ for stable motion. Based upon results reported in Ref. 6, we will assume that Eqs. (31) and (33) also apply for the longitudinal space-charge parameter μ_ℓ and the longitudinal phase advance for zero current. Thus, we will assume that the longitudinal space-charge limit occurs when $\mu_\ell = 0.84$, and that the zero current longitudinal phase advance per focusing period should not exceed $\pi/2$. In terms of the smoothed phase advance per period $\beta\lambda$ we require

$$\sigma_\ell = k_\ell\beta\lambda \lesssim \pi/2 . \tag{47}$$

We will evaluate the bunch length and radius for the longitudinal current limit just as we did for the transverse current limit. These values are given in Eqs. (28) and (30). The use of Eq. (28) for the beam radius at the longitudinal limit is a good approximation when the beam bunch is not too far from the transverse limit.

A better feeling for the explicit functional dependence of this current limit upon the parameters can be obtained by using the approximate form for the ellipsoid form factor given in Appendix A as

$$f = \frac{r}{3b} \quad . \tag{48}$$

By substituting Eqs. (48), (26), (28), and (30) into Eq. (46) we obtain the approximate result

$$I_\ell = \frac{2\mu_\ell}{Z_0} \frac{\beta E_0 T a \, \phi_s^2 \, |\sin \phi_s|}{\psi^{1/2}} \quad . \tag{49}$$

For the transit-time factor of either an Alvarez or a Wideröe linac, we use the axial transit-time expression

$$T = \frac{\sin (\pi g/\beta\lambda)}{(\pi g/\beta\lambda) I_0(2\pi a/\beta\lambda)} \quad , \tag{50}$$

where g is the accelerating gap. The quantities E_0 and T for the RFQ structure are given by Eqs. (41) and (42).

Equations 46 and 49 have the form which corresponds to the case 2 constraint discussed for the transverse current limit, when the focusing limitation is due to the magnitude of E_0, rather than the longitudinal phase advance per focusing period σ_ℓ. As can be seen from Eq. (9) large values of E_0 will increase the value of Δ_{rf}, which may greatly reduce the transverse space-charge limit as given by Eqs. (39) and (40). For large enough values of E_0, the longitudinal focusing will be limited in accordance with Eq. (47), and the form for the current limit becomes

$$I_\ell = \frac{4\pi\mu_\ell m_0 c^2 \gamma^3 r^2 b \sigma_\ell^2}{3 Z_0 e q \lambda^3 f(p)} \quad , \tag{51}$$

where we use the maximum σ_ℓ value, assumed here to be $\sigma_\ell = \pi/2$. Equation (51) corresponds to the case 1 situation, that was discussed for the transverse current limit.

IV. DISCUSSION

We have obtained some current-limit formulas for linear accelerators and have expressed them in a form that is relevant when the phase advances per focusing period at zero current are less than $\pi/2$. The transverse current limit was obtained and current-limit formulas were written for two cases. In case 1, the current was expressed in terms of a fixed phase advance σ_0, whereas for case 2 it was expressed in terms of a fixed focusing field.

Equation (35) expressed the case 1 current-limit formula. The case 2 current limit was given by Eq. (39) for magnetic focusing and by Eq. (40) for electric focusing. Equations (51) and (46) express the corresponding longitudinal space-charge limit cases.

In this report the concept of the current limit corresponds to the maximum current that can be carried through the accelerator. For the transverse case this corresponds to invoking Eqs. (33) and (34). For that current limit to be realized by a given input beam, without undue particle loss, it is necessary that the beam be matched to the accelerator and that the beam emittance not be too large. To quantify this idea, assume that the current limit is reached abruptly when the current is large enough so that $\sigma = 0.4\ \sigma_0$. The normalized acceptance of the linac can be written as

$$\alpha = \frac{a^2\sigma}{\psi L} \quad . \qquad (52)$$

From Eq. (22) we can write

$$\mu = 1 - \left(\frac{\alpha}{\alpha_0}\right)^2 \quad , \qquad (53)$$

where α_0 is the acceptance at zero beam current. Thus, as the beam current increases, both the phase advance σ and the acceptance α will decrease At the transverse current limit where $\sigma = 0.4\ \sigma_0$, $\alpha = 0.4\ \alpha_0$ results. The poor emittance case is when $\varepsilon > 0.4\ \alpha_0$. Then beam will be lost on the aperture for currents even below the limiting current. For the good emittance case, when $\varepsilon < 0.4\ \alpha_0$, the radial beam loss will be small for currents below the limiting current. In the poor emittance case, the maximum μ for a given final emittance ε is obtained by subsituting the equation $\varepsilon = \alpha$ into Eq. (53). This results in the relation given by Reiser[7] that

$$\mu = 1 - \left(\frac{\varepsilon}{\alpha_0}\right)^2 . \qquad (54)$$

The current-limit formulas given here must be evaluated at a specific energy. However, it is to be expected that a finite length of the accelerator equal to one or more cycles of transverse or longitudinal oscillation will be required to establish the current limit. Because the energy is always changing, it is difficult in a real linac to maintain a fixed value for the current limit over this distance. Even so, we have found the current-limit concept useful. From Eqs. (35) or (39) and (40) for the transverse limit, and from the approximate form of Eq. (49) for the longitudinal limit, we see that all limits increase with an increase in energy and magnitude of the synchronous phase. Because separate equations apply for the longitudinal and the transverse current limits, with different dependences upon the parameters, it is necessary to carefully specify the parameter region before making any other statements about current limit dependence on the parameters in a linear accelerator. When the longitudinal limit gives a smaller result than the transverse limit, we expect the longitudinal motion will determine the overall current limit, so that the dependence of the latter upon the parameters will be that of the longitudinal current-limit formula. Likewise, when the transverse motion sets the limit, the transverse current-limit formulas represent the overall current limit. An important intermediate case is when the transverse and longitudinal current limits are constrained to be equal. If this equality is maintained by always adjusting E_0 to compensate for the effect of varying other parameters, then E_0 depends upon these other parameters in a complicated way. The (case 2) longitudinal current limit is linearly proportional to E_0, but the transverse current limit is insensitive to E_0 when the rf defocus parameter is not too large. Therefore, for this case, the transverse current-limit formula itself gives approximately the correct explicit dependence of the overall current limit with respect to the changing parameters.

For an example we applied these current-limit formulas to an RFQ that bunches and accelerates a deuteron beam from 0.1 to 2.0 MeV with a final synchronous phase of $\phi_s = -30^0$ at an 80-MHz frequency. The design approach details are given in Ref. 3. The acceleration-efficiency parameter was kept fixed at A = 0.55 at the end of the bunching section, where both current limits occurred according to the formulas in this report. The electric field was held at a fixed value so that this example corresponds to our case 2. The curves in Fig. 1 show the calculated transverse and longitudinal current limits at the end of the bunching section as a function of θ_0^2. The rapid cutoff of the I_t curve at low θ_0^2 values is due to the rf defocus effect. The decrease of I_ℓ at large θ_0^2 values results from the decreased aperture that corresponds to large θ_0^2. The optimum operating point at

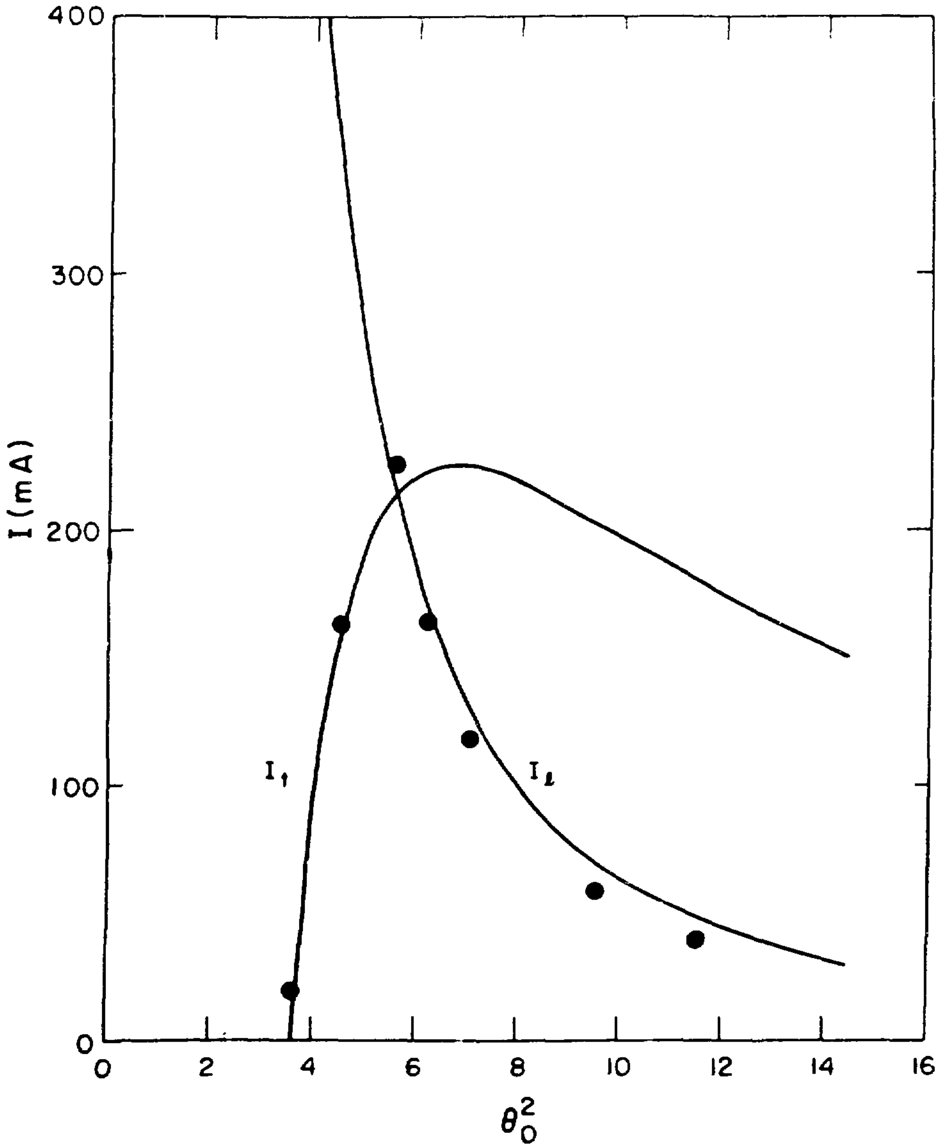

Fig. 1.
Limiting beam currents vs θ_0^2 for an RFQ. The curves are obtained from the formulas 40 and 46 given in the text. The solid points are obtained from the computer program PARMTEQ.

$\theta_0^2 = 5.6$ gives equal transverse and longitudinal limits. The data points shown in Fig. 1 are obtained from a numerical simulation using the program PARMTEQ.[3] The limiting current obtained from the PARMTEQ calculation is taken to be the saturated value of the output beam current as a function of the input current. The agreement between the data points and the lower branch of the curves is good despite the difference in the calculations. The space-charge force in PARMTEQ is treated by giving each particle one impulse per cell, which depends upon the coordinates of all other particles in the bunch. Interaction between bunches is also taken into account. In these respects and in others, the numerical calculation is done in more detail and with more realistic assumptions than the simplified ones that produced the formulas. Furthermore, many predictions of PARMTEQ have been compared with experimental measurements from the RFQ recently tested at Los Alamos Scientific Laboratory (LASL) and the agreement has been good,[8] which lends support to the PARMTEQ calculations. The formulas are not intended as a substitute for the numerical calculation, but show the dependence of the current limits on the variables in a convenient form, provide an understanding of the basic effects, which determine the maximum beam current, and serve as a guide for high-current linear accelerator design.

ACKNOWLEDGMENTS

I have benefited from discussions with R. H. Stokes, D. A. Swenson, R. A. Jameson, K. R. Crandall, G. P. Boicourt, M. Weiss, R. Gluckstern, and M. Reiser.

APPENDIX A
THREE-DIMENSIONAL ELLIPSOID MODEL

The electric field components within an azimuthally symmetric ellipsoid of radius r and longitudinal semiaxes b are given by

$$E_x = \frac{\rho x[1 - f(p)]}{2\varepsilon_0 \gamma^2} , \qquad \text{(A-1)}$$

$$E_y = \frac{\rho y[1 - f(p)]}{2\varepsilon_0 \gamma^2} \quad , \tag{A-2}$$

and

$$E_z = \frac{\rho z f(p)}{\varepsilon_0} \quad , \tag{A-3}$$

where ρ is the charge density and f(p) is the ellipsoid form factor.

The ellipsoid form factor is given in a convenient form by Gluckstern.[2] It can be written

$$f(p) = \begin{cases} \dfrac{1}{1-p^2} - \dfrac{p}{(1 - p)^{3/2}} \cos^{-1} p \;, & p < 1 \\[2ex] \dfrac{p \cosh^{-1} p}{(p^2 - 1)^{3/2}} - \dfrac{1}{\left(p^2 - 1\right)} & , \; p > 1 \;, \\[2ex] \dfrac{1}{3} & , \; p = 1 \end{cases} \tag{A-4}$$

where

$$\cosh^{-1} p = \ln\left[p + \sqrt{p^2 - 1}\right] \tag{A-5}$$

and

$$p = b/r \quad . \tag{A-6}$$

The above function is plotted in Fig. A-1 as f(p) for $p < 1$ and f(1/p) for $p > 1$. A useful approximate form is

$$f(p) \approx \frac{1}{3p} \text{ for } 0.8 < p < 5 \;. \tag{A-7}$$

The charge density can be expressed as

$$\rho = \frac{3 I \lambda}{4 \pi r^2 bc} \quad , \tag{A-8}$$

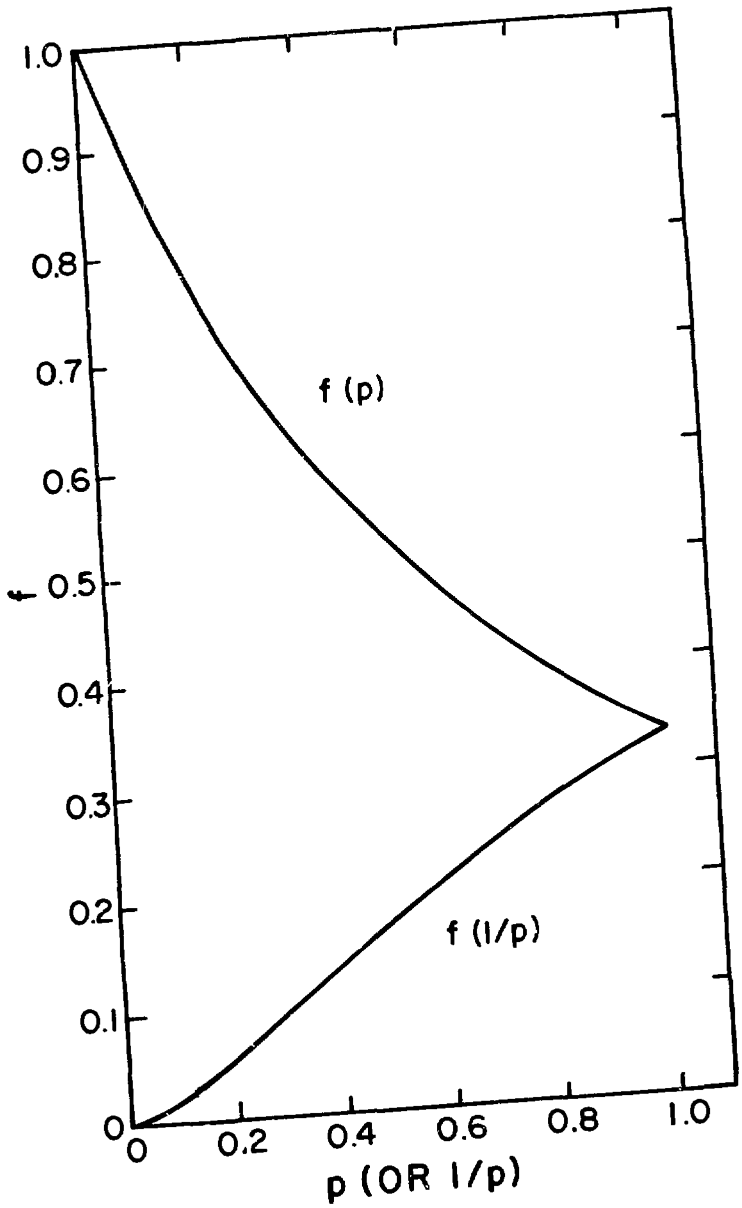

Fig. A-1.
Ellipsoid form factor f(p) vs p for $p < 1$ and f(1/p) for $p > 1$.

where I is the average beam current if all the buckets are filled, λ is the rf wavelength, and c is the speed of light. Then the field components can be written

$$E_x = \frac{3Z_0}{8\pi} \frac{I\lambda[1 - f(p)]x}{r^2 b\gamma^2} , \qquad \text{(A-9)}$$

$$E_y = \frac{3Z_0}{8\pi} \frac{I\lambda[1 - f(p)]y}{r^2 b\gamma^2} , \qquad \text{(A-10)}$$

and

$$E_z = \frac{3Z_0}{4\pi} \frac{I\lambda f(p) z}{r^2 b} , \qquad \text{(A-11)}$$

where

$$Z_0 = \frac{1}{\varepsilon_0 c} = 376.73\Omega \qquad \text{(A-12)}$$

is the impedance of free space.

APPENDIX B
MATHIEU EQUATION

We have written the Mathieu equation as

$$\frac{d^2x}{d\eta^2} + \left[\theta_0^2 \sin 2\pi\eta + \Delta\right]x = 0 , \qquad \text{(B-1)}$$

where

$$\eta = \frac{s}{L} \qquad \text{(B-2)}$$

and L is the period. Detailed information about the properties of the Mathieu equation can be found in Ref. 9. The solutions are stable or unstable

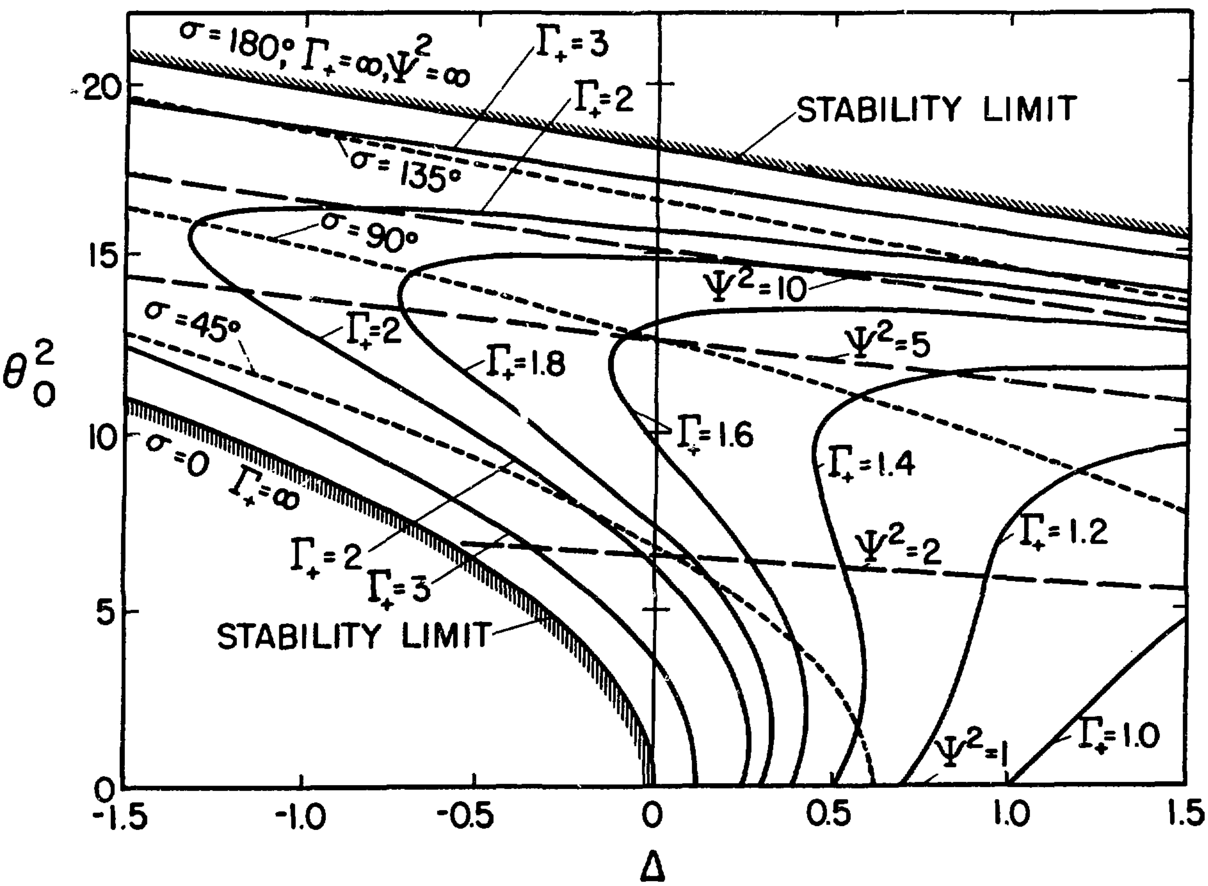

Fig. B-1.
Stability plot for Mathieu equation showing lowest stable region. The contour lines are for parameters defined in the text.

depending upon the values of the parameters θ_0^2 and Δ. For our purposes the most useful stable region is shown in Fig. B-1. The phase advance per focusing period is σ. The quantity Γ_+ is the ratio of the maximum of the betatron function to the period, or

$$\Gamma_+ = \frac{\beta_+}{L} \quad . \tag{B-3}$$

The modulation factor ψ is defined as

$$\psi = \sqrt{\frac{\beta_+}{\beta_-}} \quad . \tag{B-4}$$

Approximate formulas can be written that are often very useful. The lower stability limit in Fig. B-1 is given approximately by

$$\frac{\theta_0^4}{8\pi^2} + \Delta = 0 \quad . \tag{B-5}$$

An approximate form for the upper stability limit is

$$\left[\theta_0^2 + 2\Delta\right] = 2\pi^2 \quad . \tag{B-6}$$

The smooth approximation solution, generally valid for $\sigma < \pi/2$, gives

$$\sigma^2 = \frac{\theta_0^4}{8\pi^2} + \Delta \quad , \tag{B-7}$$

$$\Gamma_+ = \frac{\left[1 + (\theta_0/2\pi)^2\right]^2}{\sigma} \quad , \tag{B-8}$$

and

$$\psi = \frac{1 + \left(\theta_0/2\pi\right)^2}{1 - \left(\theta_0/2\pi\right)^2} \quad . \tag{B-9}$$

APPENDIX C
NOTATION

a	radial aperture
b	longitudinal semiaperture of ellipsoid

b_m	Fourier coefficient
c	speed of light
e	electron charge
f	ellipsoid form factor
g	accelerating gap
k	longitudinal wave number
k_t	transverse wave number
m	mth Fourier component
m_0	particle mass
p	aspect ratio of ellipsoid
q	charge state of ion
r	radius of ellipsoid (mean beam-envelope radius)
r_+	maximum envelope radius
r_-	minimum envelope radius
r_x	beam-envelope radius
s	coordinate along accelerator axis
x	transverse coordinate of particle
y	transverse coordinate of particle
A	acceleration efficiency
A_n	atomic mass number of ion
B	magnetic flux density
E_0	average axial electric field amplitude
I	average beam current assuming all buckets are filled
I	longitudinal current limit
I_t	transverse current limit
L	length of focusing period
N	ratio of focusing period to $\beta\lambda$
T	transit-time factor
V	intervane voltage
X	slowly varying factor in smooth approximation solution
Z_0	free-space impedance, 376.73 Ω
α	transverse acceptance
α_0	transverse acceptance at zero beam current
β	ratio of particle velocity to speed of light
β_+	maximum betatron function
β_-	minimum betatron function

β_x betatron function

β_x mean betatron function

γ ratio of total particle energy to m_0c^2

Γ_+ ratio of maximum betatron function to focusing period

δ phase of betatron motion

Δ total defocusing parameter

Δ_{rf} rf defocusing parameter

Δ_{sc} space-charge defocusing parameter

ε emittance, ratio of beam phase-space area to π

ε_0 permitivity of free space

η ratio of axial coordinate to focusing period

θ_0 quadrupole focusing parameter

λ rf wavelength

Λ quadrupole filling factor

μ longitudinal space-charge parameter

μ_t transverse space-charge parameter

ρ charge density

σ transverse phase advance per focusing period

σ_0 transverse phase advance per focusing period at zero current

σ_ℓ longitudinal phase advance per focusing period

ϕ particle phase

ϕ_s synchronous phase

χ focusing efficiency factor

ψ betatron function modulation ratio

Ω symbol for ohms

REFERENCES

1. A. Maschke, "Space-Charge Limits for Linear Accelerators," Brookhaven National Laboratory report BNL 51022, (May 1, 1979).

2. R. L. Gluckstern, "Space-Charge Effects," in Linear Accelerators, P. M. Lapostolle and A. L. Septier, Eds. (North Holland Publishing Co., Amsterdam, 1970).

3. K. R. Crandall, R. H. Stokes, and T. P. Wangler, "RF Quadrupole Beam Dynamics Design Studies," Proc. of the 1979 Linear Accelerator Conference, Montauk, New York, September 9-14, 1979.

4. I. M. Kapchinskii and V. A. Teplyakov, "Linear Ion Accelerator with Spatially Homogeneous Strong Focusing," Prib. Tekh. Eksp. No. 2, 19 (1970).

5. H. Bruck, "Circular Particle Accelerators," English translation in Los Alamos Scientific Laboratory report LA-TR-72-10 Chapter IX.

6. R. A. Jameson and R. S. Mills, "On Emittance Growth in Linear Accelerators," Proc. of the 1979 Linear Accelerator Conference, Montauk, New York, September 9-14, 1979.

7. M. Reiser, "Periodic Focusing of Intense Beams," Part. Accel. 8, 167-182 (1978).

8. R. W. Hamm, K. R. Crandall, L. D. Hansborough, J. M. Potter, G. W. Rodenz, R. H. Stokes, J. E. Stovall, D. A. Swenson, T. P. Wangler, C. W. Fuller, M. D. Machalek, R. A. Jameson, E. A. Knapp, and S. W. Williams, "The rf Quadrupole Linac: A New Low-Energy Accelerator," submitted to Int. Conf. on Low-Energy Ion Beams 2, University of Bath, Bath, England, April 14-17, 1980.

9. M. Abramowitz and I. A. Stegun, "Handbook of Mathematical Functions," National Bureau of Standards, Applied Mathematics Series AMS 55, 1964, p. 721.

☆U.S. GOVERNMENT PRINTING OFFICE: 1980—777-022/215